

Influence of Ester Functional Groups on the Liquid-Phase Structure and Solvation Properties of Imidazolium-Based Ionic Liquids

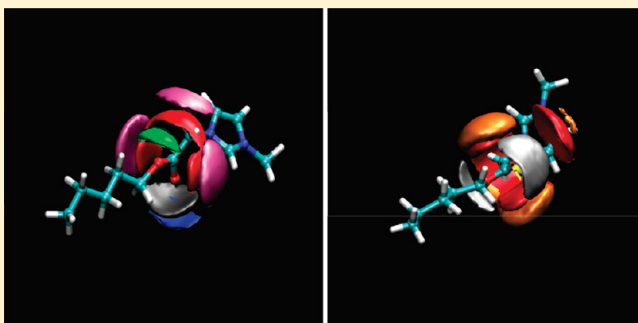
Alfonso S. Pensado,^{†,§} Agílio A. H. Pádua,^{†,‡} and Margarida F. Costa Gomes^{*,†,‡}

[†]Laboratoire Thermodynamique et Interactions Moléculaires, Clermont Université, Université Blaise Pascal, BP 80026, 63171 Aubiere, France

[‡]CNRS, UMR6272 LTIM, BP 80026, 63171 Aubiere, France

[§]Laboratorio de Propiedades Termofísicas, Departamento de Física Aplicada, Universidade de Santiago de Compostela, E-15782, Santiago de Compostela, Spain

ABSTRACT: The incorporation of ester functions in the side chains in 1-alkyl-3-methylimidazolium cations seems to increase the biodegradability of these ionic liquids. We study here how the presence of ester functional groups affects the liquid-state structure (namely, the microphase segregation between polar and nonpolar domains in these ionic liquids) and the way in which the solvation of gases can be understood in these solvents. We use molecular simulation to study the structure of the ionic liquids 3-methyl-1-(pentoxycarbonylmethyl)imidazolium octylsulfate, $[\text{C}_1\text{COOC}_5\text{C}_1\text{im}][\text{C}_8\text{SO}_4]$; and 3-methyl-1-(pentoxycarbonylmethyl)imidazolium bis-(trifluoromethylsulfonyl)imide, $[\text{C}_1\text{COOC}_5\text{C}_1\text{im}][\text{NTf}_2]$ in the liquid phase and to assess the molecular mechanisms of solvation of carbon dioxide and ethane. The presence of ester functions influences the relative size of the polar and nonpolar domains in the ionic liquids, but does not significantly affect the solvation of gases.



INTRODUCTION

Room temperature ionic liquids (RTILs) are salts with melting points below 373 K. They have attracted considerable interest in many fields of chemistry and in the chemical industry; namely, to replace conventional organic solvents used in chemical and catalytic reactions, separations, and purifications.^{1,2} Ionic liquids are also suitable as lubricants;^{3,4} in electrochemical applications, such as solar cells;⁵ and nanotechnology.^{6,7} The low vapor pressure, which minimizes the environmental impact; the low flammability; and the wide liquid temperature range in conjunction with thermal stability are key properties for the growing interest in ILs for many applications. Ionic liquids have been considered as “green solvents” even if their biodegradability is low⁸ and the toxicity in the environment, high.^{9–11}

Ionic liquids are modular, since chemical structural modifications can be made either in the anion, the cationic core, or substituents on the anion or cation. The physicochemical properties of ionic liquids can be adjusted in view of particular applications, and new compounds, termed “task specific ionic liquids” (TSIL) may be synthesized. Physical properties that can be tailored to the requirements of a process include the melting point, viscosity, density, solubility, and hydrophobicity. Moreover, reaction products may be separated more easily from an ionic liquid than from conventional solvents. Gathergood and Scammells⁸ used the concept of TSIL and showed that the introduction of ester groups, which are susceptible to enzymatic

hydrolysis, in the alkyl side chains of methylimidazolium-based ionic liquids greatly improves the degradability of these compounds.

A recent review by Coleman and Gathergood¹² presents an overview of studies into the biodegradability of ionic liquids, including the various methods of biodegradation assessment, trends observed for structurally related ionic liquids, and applications of biodegradable ionic liquids in synthetic chemistry. These authors state that because of the vastness of the library of ionic liquids that might be synthesized, it is important to consider at the design stage the factors that may influence the toxicity and biodegradation of ionic liquids. The work of Boethling et al.^{13,14} on the design of biodegradable chemicals has greatly assisted researchers in the field of ionic liquids by laying down guidelines for the synthesis of environmentally benign solvents. These authors emphasized different factors that can improve mineralization of organic compounds by mixed microbial communities, but these “rules of thumb” are only guidelines, and the presence of a single desirable or undesirable motif within a molecule does not guarantee either biodegradability or persistence in the environment.

The design of biodegradable ionic liquids requires a balance between the required stability as a solvent and favorable

Received: November 12, 2010

Revised: January 18, 2011

Published: March 10, 2011

biodegradability. Such considerations are especially important if specific functional groups introduced into the ionic liquid to improve its biodegradation hinder its practical applications. Only a few publications have investigated the potential of known biodegradable ionic liquids as new solvents.

Bouquillon et al.¹⁵ described a selective hydrogenation of 1-phenoxyoctadiene in which reduction of the terminal double bond occurs as the major process, leaving the internal olefin intact. Several ionic liquids were screened as solvents, and the highest conversion for the hydrogenation of 1-phenoxyocta-2,7-diene was obtained using $[\text{C}_1\text{COOC}_5\text{C}_1\text{im}][\text{C}_8\text{SO}_4]$ as the solvent (85% conversion), with the desired product, 1-phenoxyoct-2-ene, obtained with a 70% yield. This reaction offers a clear example of how a biodegradable solvent can replace a conventional one, actually giving an improvement in performance. Morrissey et al.¹⁶ analyzed a range of imidazolium ionic liquids with ester groups in the side chain as reaction solvents for selective hydrogenation where trans-cinnamaldehyde was reduced to hydrocinnamaldehyde. Selectivities toward hydrocinnamaldehyde ranged from 90 to 100% when the imidazolium pentyl esters $[\text{C}_1\text{COOC}_5\text{C}_1\text{im}][\text{NTf}_2]$ and $[\text{C}_1\text{COOC}_5\text{C}_1\text{im}][\text{NTf}_2]$ were employed as the reaction media.

Deng et al.¹⁷ studied the influence of the introduction of ester or ether groups on the alkyl side chains of the imidazolium ring of the cation and of two different anions (bis(trifluoromethylsulfonyl)imide and octyl sulfate) on the density and the solubility of four gases (carbon dioxide, ethane, methane, and hydrogen). They concluded that the gas solubilities are of the same order of magnitude as those determined for alkylimidazolium ionic liquids; therefore, the chemical modification of the alkyl side chain does not introduce a significant change in the solvation properties of the ionic liquid.

Herein, we use molecular simulation to study the nanoscale structuring of the ionic liquids 3-methyl-1-(pentoxycarbonylmethyl)imidazolium octylsulfate, $[\text{C}_1\text{COOC}_5\text{C}_1\text{im}][\text{C}_8\text{SO}_4]$, and 3-methyl-1-(pentoxycarbonylmethyl)imidazolium bis(trifluoromethylsulfonyl)imide, $[\text{C}_1\text{COOC}_5\text{C}_1\text{im}][\text{NTf}_2]$, in the liquid phase and to assess the molecular mechanisms of solvation of carbon dioxide and ethane. The choice of these two gases was based not only on their technological and environmental importance but also on fundamental aspects due to differences in their interactions: those of CO_2 with ionic liquids are dominated by the quadrupole moment of the gas¹⁸ (a type of polarity), whereas those of C_2H_6 are essentially nonpolar interactions.

SIMULATION METHODOLOGY

Potential Model. Ionic liquids were represented by an all-atom force field,^{19,20} which is based on the AMBER/OPLS_AA framework^{21,22} but was developed specifically for ionic liquids. This model contains all the parameters required to simulate the ions $[\text{C}_8\text{SO}_4]^-$, $[\text{NTf}_2]^-$, and the imidazolium cations with ester-functionalized alkyl side chains (Figure 1). The functional form of the force field contains four kinds of potential energy: stretching of covalent bonds, bending of valence angles, torsion around dihedral angles, and nonbonded interactions. Nonbonded interactions are active between atoms of the same molecule separated by more than three bonds and between atoms of different molecules. The potential energy associated with bonds and angles is described by harmonic terms, dihedral torsion energy is represented by series of cosines, and nonbonded interactions are given by the Lennard-Jones sites and by Coulomb

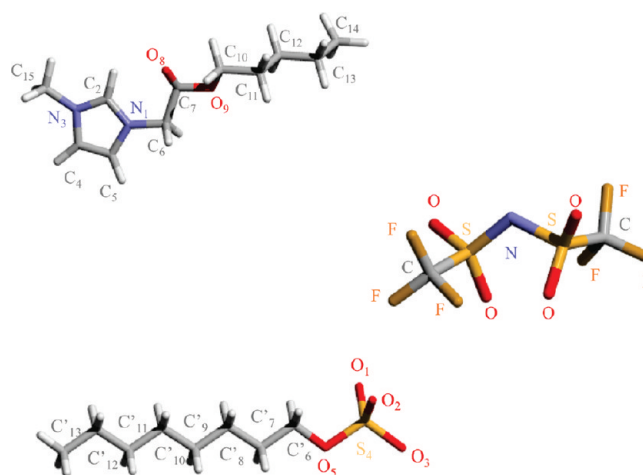


Figure 1. Adopted nomenclature for the sites of the ionic liquids 1-methyl-3-(pentoxycarbonylmethyl)imidazolium octylsulfate and 1-methyl-3-(pentoxycarbonylmethyl)imidazolium bis(trifluoromethylsulfonyl)imide.

interactions (calculated using the Ewald summation method) between partial point charges placed on the atomic sites.

Computational Procedures. The ionic liquids $[\text{C}_1\text{COOC}_5\text{C}_1\text{im}][\text{C}_8\text{SO}_4]$ and $[\text{C}_1\text{COOC}_5\text{C}_1\text{im}][\text{NTf}_2]$ were simulated in periodic cubic boxes containing 256 ion pairs, using the molecular dynamics method implemented in the DL_POLY package.²³ The initial configurations were lattices with low density. Equilibrations starting from the low density arrangement of ions took 500 ps, at constant NpT and $T = 423$ K, with a time step of 2 fs. Once the equilibrium density was obtained, simulation runs of 1 ns were performed. At the final densities of the ionic liquid state, the length of the sides of the simulation boxes is ~ 54 and 56 Å for the ionic liquids with the $[\text{NTf}_2]^-$ and $[\text{C}_8\text{SO}_4]^-$ anion, respectively. To analyze the possible effect of the box size, independent simulations were performed on systems containing 512 ion pairs at the same conditions. The length of the side of the simulation boxes is approximately 67 and 70 Å for the ionic liquids with the $[\text{NTf}_2]^-$ and $[\text{C}_8\text{SO}_4]^-$ anion, respectively. In addition, simulation boxes containing 246 ion pairs and 4 CO_2 or C_2H_6 molecules were prepared to calculate solute–solvent radial distribution functions between the gas and the ionic liquid. We selected this reduced number of solute molecules to avoid solute–solute interactions but still obtain a good sampling of the condensed phase structure. The potential model of Harris and Yung²⁴ was used for CO_2 , whereas the parameters for C_2H_6 were those of the OPLS_AA model.^{21,22}

The chemical potentials of CO_2 and C_2H_6 at 373 K in the two ionic liquids were calculated in a two-step procedure, similar to that used recently by Almantariotis et al.²⁵ to obtain this quantity in the ionic liquids $[\text{C}_8\text{C}_1\text{im}][\text{NTf}_2]$ and $[\text{C}_8\text{F}_{13}\text{H}_4\text{C}_1\text{im}][\text{NTf}_2]$. First, for CO_2 , a reduced-size version of the molecule was produced by subtracting 0.8 Å from the C–O bond length and also from the Lennard-Jones diameters σ_{O} and σ_{C} . For C_2H_6 , the initial molecule had C–H and C–C bond lengths of 0.4 and 0.529 Å, respectively, whereas the Lennard-Jones diameters σ_{C} and σ_{H} were reduced in 1 Å. The resulting molecules are small enough that their chemical potentials can be calculated using the Widom²⁶ test-particle insertion method with efficient statistics. The difficulty with the test-particle insertion method is that free volume in ionic liquids is low, and spontaneously

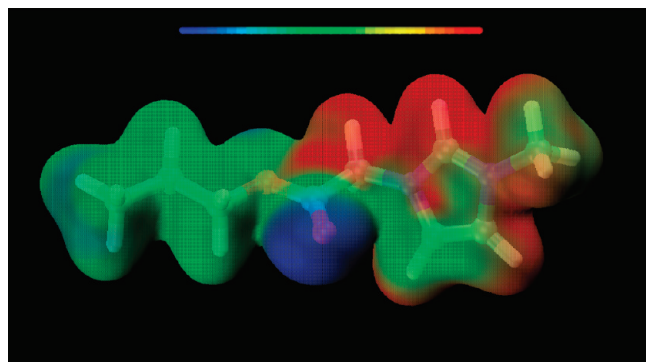


Figure 2. Mapping of the electrostatic potential onto an isoelectronic density surface obtained ab initio at the MP2/cc-pVTZ(-f) level, thus including electron correlation and using a suitable extended basis set (darker red shades represent more positive regions and darker blue represent more negative regions) in the $[\text{C}_1\text{COOC}_5\text{C}_1\text{im}]^+$ cation. The basis set is created by removing the f functions from the cc-pVTZ basis set.⁴⁶ Details of the calculations can be found in the literature.¹⁹

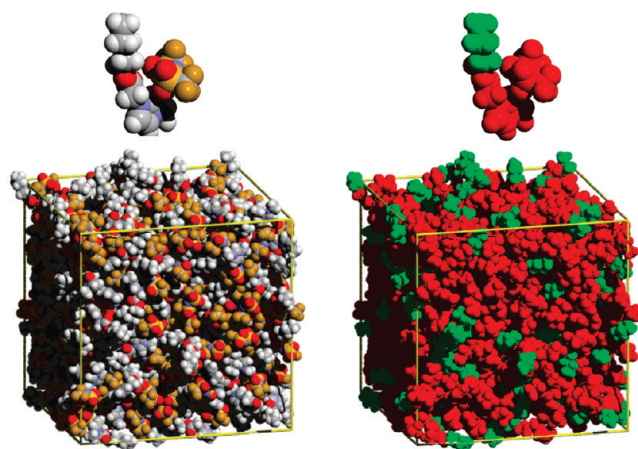


Figure 3. Snapshots of the simulation box of $[\text{C}_1\text{COOC}_5\text{C}_1\text{im}][\text{NTf}_2]$.

present cavities capable of accommodating a full CO_2 or C_2H_6 molecule are very unlikely to occur, resulting in a practical difficulty to calculate the chemical potential of these gases by direct test-particle insertion. Simulation runs of 600 ps at 373 K were performed, from which 3000 configurations were stored. Then, 10^5 insertions were attempted in each of the 3000 stored configurations of the pure ionic liquids.

Second, a stepwise finite difference thermodynamic integration procedure²⁷ was used to calculate the free-energy difference between the initial, reduced versions of the carbon dioxide and ethane molecules and the full-size model. The free energy calculation was performed on six intermediate steps along a linear path connecting the intermolecular parameters (bonds and diameters) of the reduced-size to those of the full-size molecule. We selected this moderately modest number of intermediate steps because the starting point and the final state of the thermodynamic integration route are not too far. If we intend to calculate the chemical potential of CO_2 or C_2H_6 by thermodynamic integration starting from the pure solvent, then a large number of intermediate steps would be required. In the finite-difference thermodynamic integration scheme, derivatives (finite differences) of the total energy of the system with respect to the

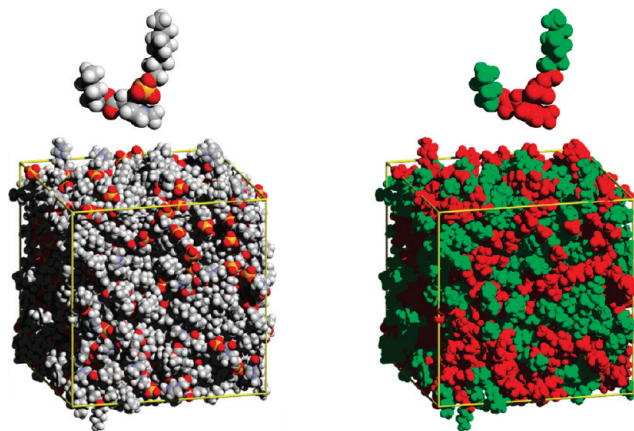


Figure 4. Snapshots of the simulation box of $[\text{C}_1\text{COOC}_5\text{C}_1\text{im}][\text{C}_8\text{SO}_4]$.

activation parameter were evaluated by a free-energy perturbation expression in the NpT ensemble using a three-point formula with increments of 2×10^{-3} . We have selected the temperature of 373 K to minimize the sampling problems related to the slow dynamics of the ionic liquids.²⁸

RESULTS AND DISCUSSION

To validate the force field and the simulation methodology used, we have compared the values of the density of the pure ionic liquids at 373 K, obtained by molecular simulation, with those determined experimentally by Deng et al.¹⁷ Deng et al. have proposed an equation to correlate the experimental densities of the ionic liquids $[\text{C}_1\text{COOC}_5\text{C}_1\text{im}][\text{C}_8\text{SO}_4]$ and $[\text{C}_1\text{COOC}_5\text{C}_1\text{im}][\text{NTf}_2]$ that we have used to extrapolate the experimental values to 373 K, the temperature at which the molecular simulation were made in this work. The deviations encountered are +3.8% and −5.0% for the ILs with the $[\text{NTf}_2]^-$ and $[\text{C}_8\text{SO}_4]^-$ anions, respectively. These deviations are similar to those obtained by Canongia Lopes et al.¹⁹ when the characteristic parameters of the force field to represent the alkoxycarbonyl imidazolium cations and the alkylsulfate anions were determined. An accuracy of around 3% in liquid densities is reasonable and justified by the generality and transferability of the force field model.

Polar and Nonpolar Domains. Wang and Voth,²⁹ using a multiscale coarse-graining (MS-CG) method, and Canongia Lopes and Pádua,³⁰ using an all-atom potential model, reported the existence of a nanometer-scale structuring in imidazolium-based ionic liquids (from $\text{C}_2\text{C}_1\text{im}$ to $\text{C}_{12}\text{C}_1\text{im}$) corresponding to a segregation of polar and nonpolar domains. Triolo et al.^{31–33} provided experimental evidence, using X-ray diffraction, of the existence of a nanoscale organization in the ionic liquids of the families $[\text{C}_n\text{C}_1\text{im}][\text{PF}_6]$, $[\text{C}_n\text{C}_1\text{im}][\text{BF}_4]$, $[\text{C}_n\text{C}_1\text{im}][\text{Cl}]$, and $[\text{C}_n\text{C}_1\text{im}][\text{NTf}_2]$. This segregation into ionic and nonpolar spatial domains is important to define the solvation characteristics of ionic liquids, through effects of this dual structure and also through the types of interaction with polar and nonpolar solutes.³⁴

We analyze the microscopic structure of imidazolium-based ionic liquids with ester functionalized alkyl chains. We adopted the coloring code proposed by Canongia Lopes and Pádua³⁰ to identify high-charge- (red) and low-charge-density (green) regions. The four terminal carbon atoms of the alkyl chains of the cations (and the hydrogen atoms bonded to them), the seven

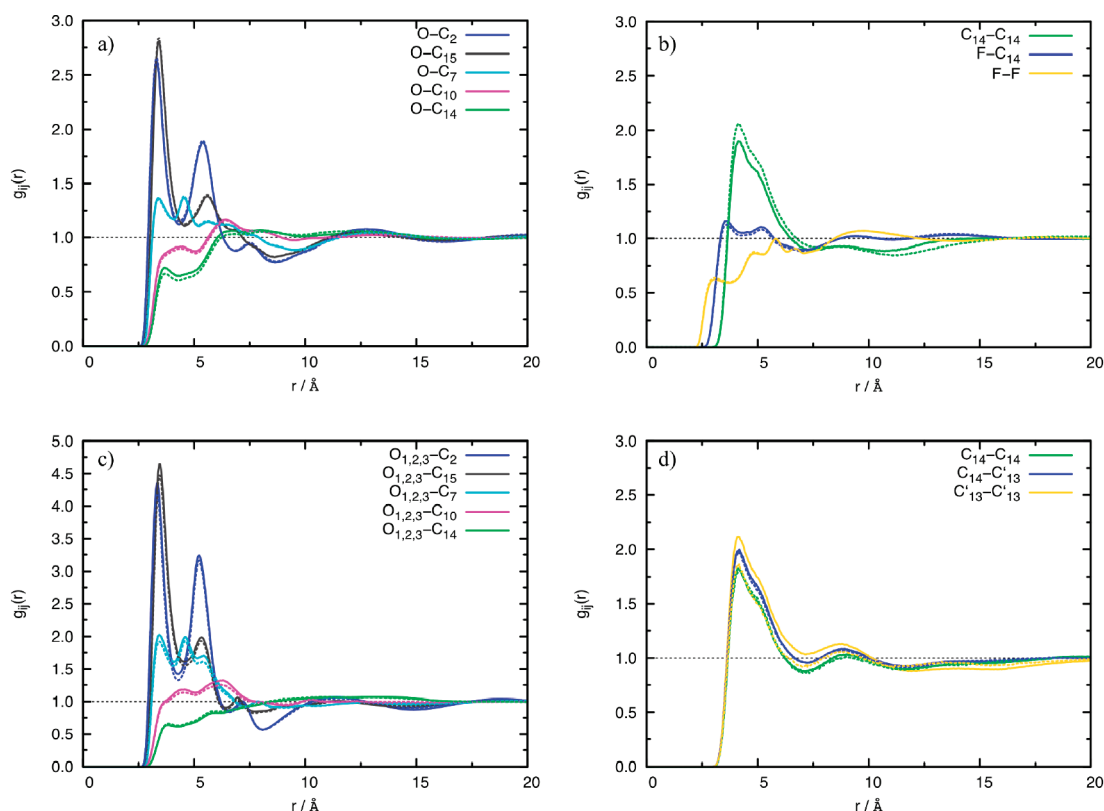


Figure 5. Cation–anion site–site radial distribution functions (RDFs). Solid lines are the results obtained considering 256 ion pairs, and dashed lines represent those obtained considering 512 ion pairs. (a) Oxygen atoms of the $[\text{NTf}_2]^-$ anion around the $[\text{C}_1\text{COOC}_5\text{C}_1\text{im}]^+$ cation. (b) Terminal carbon atoms of the alkyl chain of the $[\text{C}_1\text{COOC}_5\text{C}_1\text{im}]^+$ cation, and Fluor atoms of the $[\text{NTf}_2]^-$ anion. (c) Oxygen atoms of the $[\text{C}_8\text{SO}_4]^-$ anion around the $[\text{C}_1\text{COOC}_5\text{C}_1\text{im}]^+$ cation. (d) Terminal carbon atoms of the alkyl chain of the $[\text{C}_1\text{COOC}_5\text{C}_1\text{im}]^+$ cation and the $[\text{C}_8\text{SO}_4]^-$ anion. The names of the atoms correspond to those presented in Figure 1.

terminal carbon atoms, and the bonded hydrogen atoms of the octylsulfate anion constitute the regions considered to be of low charge density. The atoms of the $[\text{NTf}_2]^-$ anion, those of the imidazolium ring, plus atoms bonded to them (including hydrogen atoms bonded to the first carbon of the alkyl chain) and the atoms of the ester group constitute the regions considered to be of high charge density. The justification for such a division is illustrated in the electrostatic surface potential plot in Figure 2. Examples of the simulation boxes containing the two ionic liquids are shown in Figures 3 and 4. We also present in these figures the color code used to distinguish the “polar” and “nonpolar” regions. The morphology of the polar and nonpolar regions presented in this functionalized IL is similar to that observed in alkylimidazolium ionic liquids. The relative sizes of the polar and nonpolar domains in the two ionic liquids herein depend on the size of the anion, the long alkyl chain of the octylsulfate leading to larger nonpolar regions.

We present in Figure 5 site–site radial distribution functions between several representative atoms of the anion and cation of both ionic liquids. As stated above, the present simulations were performed with 256 and 512 ion pairs, and the structural information obtained from the two system sizes are comparable. The most prominent feature of the radial distribution functions is the strong correlation between the oxygen atoms of the anions $[\text{NTf}_2]^-$ and $[\text{C}_8\text{SO}_4]^-$ (where the negative charge is concentrated) and atoms of the imidazolium rings. These O atoms of the anions are also found with significant probability in the vicinity of the ester function of the cation, as can be observed in

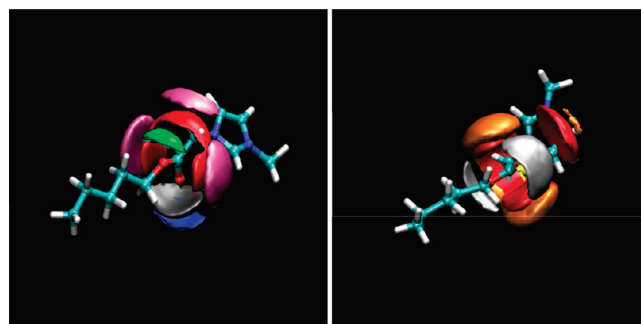


Figure 6. Spatial distribution functions around the ester group of the cation in the liquids $[\text{C}_1\text{COOC}_5\text{C}_1\text{im}][\text{NTf}_2]$ (left) and $[\text{C}_1\text{COOC}_5\text{C}_1\text{im}][\text{C}_8\text{SO}_4]$ (right). Left panel: Carbon C_2 in the imidazolium ring (blue), carbon C_{15} of the alkyl chain (gray), terminal carbon of the alkyl chain of the cation C_{14} (green), oxygen atoms of the anion O (red), and nitrogen of the anion N (purple). Right panel: Carbon C_{15} of the alkyl chain (gray), oxygen atoms of the anion O_5 (orange), and oxygen atoms of the anion $\text{O}_{1,2,3}$ (red). The isosurfaces correspond to three times the average density.

panels a and c of Figure 5. Panel b shows a strong first peak in the radial distribution functions of the terminal carbon atoms of the alkyl chain of the cation in the liquid $[\text{C}_1\text{COOC}_5\text{C}_1\text{im}][\text{NTf}_2]$.

For the ionic liquid $[\text{C}_1\text{COOC}_5\text{C}_1\text{im}][\text{C}_8\text{SO}_4]$, panel d of Figure 5 shows a comparison of radial distribution functions of the terminal carbon atoms of the cation and anion. The most outstanding feature is that both terminal atoms of cations and

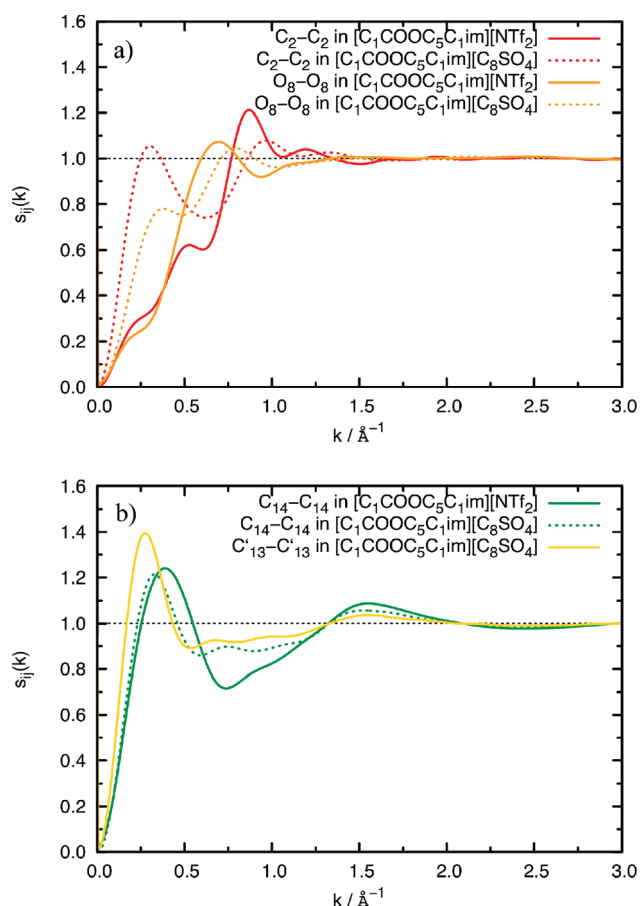


Figure 7. Static structure factors of representative atoms of the polar and apolar regions calculated from radial distribution functions.

anions were found with a high probability at close distances, which is a sign of alkyl-chain aggregation. For the ionic liquid with the octylsulfate anion, the alkyl chains of cations and anions form the nonpolar region. More precise structural features are better observed in the 3-dimensional spatial distribution functions, shown in Figure 6. We can observe that there is a high probability of finding the anions of both ionic liquids near the ester group of the cation. The presence of the ester group in the cation adds a second charged region to the cation, so there is a competition between the imidazolium ring and the ester group to attract the anion, causing a modification in the ordering present in these ionic liquids when compared with what is observed in the nonfunctionalized alkyl imidazolium.

To characterize the length scales of the polar and nonpolar regions, we can use the static partial structure factors,³⁰ $s_{ij}(k)$ corresponding to the partial RDFs, $g_{ij}(r)$, that were defined by Fourier transform according to eq 1, where ρ is the number density of the atomic sites considered.

$$S_{ij}(k) = 1 + \frac{4\pi\rho}{k} \int_0^\infty [g_{ij}(r) - 1] r \sin(kr) dr \quad (1)$$

The results for the partial structure factors of several representative sites of the polar and nonpolar regions are presented in Figure 7. Prepeaks in the structure factors indicate the presence of characteristic lengths that are larger than first-neighbor ion-ion contacts. Such prepeaks have been observed (by both simulations³⁰ and experiments^{31–33}) in ionic liquids with alkyl side chains of intermediate length, indicating aggregation of the

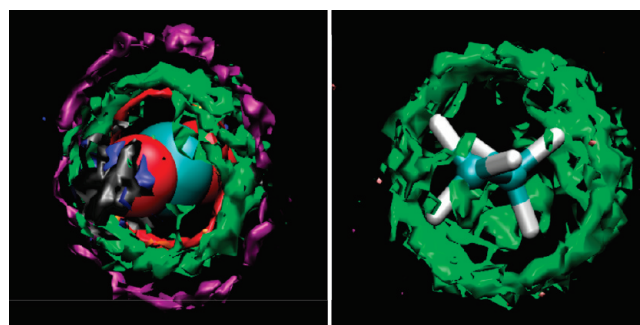


Figure 8. Probability distribution of $[C_1COOC_5C_1im][NTf_2]$ around CO_2 (left) and C_2H_6 (right). Carbon C_2 of the imidazolium ring (blue), carbon C_{15} of the alkyl chain (gray), end carbon of the alkyl chain C_{14} (green), oxygen atoms of the anion O (red), and nitrogen of the anion N (purple).

chains into nonpolar domains, while the charged head groups of the ions keep in close contact. The origin of such prepeaks has been analyzed recently in great detail.⁴⁷ The partial structure factors concerning the C_2 atoms of the cation head groups and the carbonyl O atoms (shown in panel a of Figure 7) contain several peaks that are related to separations among imidazolium groups and ester groups, respectively. The picture is complicated by the possibility of different positions for nearest neighbors due to the asymmetry of the cation, as can be seen from the spatial distribution functions of Figure 6, and by the long-range ordering of ionic fluids. In addition, the continuity of ion-counterion contacts in the liquid phase means that the most evident manifestation of side-chain aggregation is not easily seen in these partial structure factors.

A more clear picture can be observed if we represent the partial structure factors of the terminal carbon atoms of the alkyl chain of the cation and of the $[C_8SO_4]^-$ anion, which give us an indication of the size of the nonpolar domains. Panel b of Figure 7 shows broad peaks at 1.5 \AA^{-1} (distances around 4 \AA) that correspond to close intermolecular distances of side chains, and strong peaks at 0.38 \AA^{-1} corresponding to a wavelength of around 16.2 \AA for the IL and at 0.33 and 0.28 \AA^{-1} ($\lambda = 19$ and $\lambda = 22.6 \text{ \AA}$) for $[C_1COOC_5C_1im][C_8SO_4]$. The nonpolar domains are therefore larger in the IL with the $[C_8SO_4]^-$ anion. The domains' length compare the results of Figure 7 with the snapshots of Figures 3 and 4. The different morphology of the polar and nonpolar domains in these two ionic liquids can influence the solvation of different species and thus probably also the performance of these liquids as reaction or separation media.

Solvation of Gases. A number of investigations, including molecular simulations^{35,36} and experiments,^{37–39} have shown that the nature of anions dominates the interaction between CO_2 and ILs. Recently, Almantariotis et al.²⁵ demonstrated that it is possible to increase by 20% the solubility of CO_2 through partial fluorination of the alkyl chain in an octylimidazolium-based ionic liquid. Several articles, using both experimental and molecular simulation techniques, show that the nature of the cation also plays an important role in the solubility of CO_2 , so both the nature of the anion and the cation influence the solubility of carbon dioxide in ionic liquids.^{36,40–44}

Costa Gomes et al.⁴⁵ studied the solvation of ethane and butane in the family of $[C_nC_1im][NTf_2]$ both experimentally and by molecular simulation, observing an increase in the gas solubility of C_2H_6 when the length of the alkyl chain of the

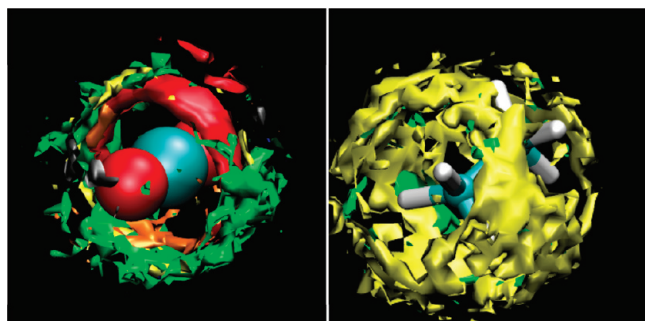


Figure 9. Probability distribution of $[\text{C}_1\text{COOC}_5\text{C}_1\text{im}][\text{C}_8\text{SO}_4]$ around CO_2 (left) and C_2H_6 (right). Carbon C_2 of the imidazolium ring (blue), carbon C_{15} of the alkyl chain (gray), end carbon of the alkyl chain C_{14} (green), oxygen atoms of the ester group O_8 (orange), oxygen atoms of the anion $\text{O}_{1,2,3}$ (red), and end carbon of the alkyl chain $\text{C}_{13'}$ (anion) (yellow).

imidazolium cation increases. The molecular simulation results indicate that ethane interacts preferentially with the nonpolar region of the ionic liquids. Short-range ordering in liquids is usually represented by site–site radial distribution functions, the spatial distribution functions giving a better perception of local structure. Figure 8 shows the probability distribution of the ionic liquid $[\text{C}_1\text{COOC}_5\text{C}_1\text{im}][\text{NTf}_2]$ around carbon dioxide and ethane, whereas in Figure 9, it is possible to observe the distribution of $[\text{C}_1\text{COOC}_5\text{C}_1\text{im}][\text{C}_8\text{SO}_4]$ around the gas molecules. CO_2 interacts preferentially with the oxygen atoms of the $[\text{NTf}_2]^-$ and $[\text{C}_8\text{SO}_4]^-$ anions but also with the terminal C atom of the alkyl chain of the cation in both ionic liquids $[\text{C}_1\text{COOC}_5\text{C}_1\text{im}][\text{NTf}_2]$ and $[\text{C}_1\text{COOC}_5\text{C}_1\text{im}][\text{C}_8\text{SO}_4]$. The behavior observed is quite similar to that observed recently by Almantariotis et al.²⁵ in $[\text{C}_n\text{C}_1\text{im}][\text{NTf}_2]$ ionic liquids. In the ionic liquid with the octylsulfate anion, CO_2 interacts also with the polar ester group. This is related to the stronger interaction between the ester group and the $[\text{C}_8\text{SO}_4]^-$ anion observed in Figure 5, as compared with the $[\text{NTf}_2]^-$ anion (the peaks in the RDFs are more intense in the former case). C_2H_6 is solvated near the alkyl chains of the cation and also near the alkyl chains of the octylsulfate anion. We do not observe any specific interaction of this gas with the polar regions of the ILs.

CO_2 and C_2H_6 Solubilities in the Ionic Liquids. Calculations of the free energy of solvation of CO_2 and C_2H_6 in the ionic liquids $[\text{C}_1\text{COOC}_5\text{C}_1\text{im}][\text{NTf}_2]$ and $[\text{C}_1\text{COOC}_5\text{C}_1\text{im}][\text{C}_8\text{SO}_4]$ at 373 K give access to the Henry's law constants, K_{H} , that allow us to calculate the gas solubility at a partial pressure of gas $p_{\text{gas}} = 1$ bar. The results are summarized in Figure 10, where a comparison with the experimental values of Deng et al.¹⁷ is also presented. The results of our simulations agree with the experiments. Both simulation and experiments indicate that CO_2 is more soluble than C_2H_6 in both ionic liquids. Our results also show that carbon dioxide is more soluble in the IL with the $[\text{NTf}_2]^-$ anion, whereas C_2H_6 is more soluble in the IL with the $[\text{C}_8\text{SO}_4]^-$ anion, in agreement with the observed experimental trends.

The solubility of the two gases can be explained by the relative sizes of the domains in the two ILs: C_2H_6 is more soluble in the IL that exhibits larger nonpolar domains. We observed a better agreement between the values of solubility of carbon dioxide in the two ionic liquids obtained experimentally and by molecular simulation. The value of the gas solubility of CO_2 in the IL

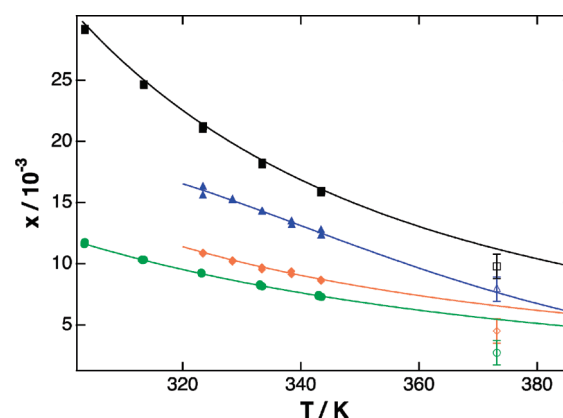


Figure 10. Mole fraction gas solubilities at 0.1 MPa partial pressure of the solutes as a function of the temperature. Solid symbols are experimental results,¹⁷ and open symbols are molecular simulation calculations, whereas the lines represent the correlation of the experimental values proposed by Deng et al.¹⁷ Black \blacksquare , CO_2 in $[\text{C}_1\text{COOC}_5\text{C}_1\text{im}][\text{NTf}_2]$; green \bullet , C_2H_6 in $[\text{C}_1\text{COOC}_5\text{C}_1\text{im}][\text{NTf}_2]$; blue \blacktriangle , CO_2 in $[\text{C}_1\text{COOC}_5\text{C}_1\text{im}][\text{C}_8\text{SO}_4]$; and orange \blacklozenge , C_2H_6 in $[\text{C}_1\text{COOC}_5\text{C}_1\text{im}][\text{C}_8\text{SO}_4]$.

$[\text{C}_1\text{COOC}_5\text{C}_1\text{im}][\text{C}_8\text{SO}_4]$ is quite close to the experimental one. In the case of ethane, we can claim only that molecular simulation provides qualitative information about the trend of gas solubility with the molecular structure of the ILs. Nevertheless, we can conclude that molecular simulation allows reproduction of the correct tendencies of gas solubility with the molecular structure, so it can be used as a tool to inspect different molecular structures of ionic liquids and provide information about the gas solubility, even if there are some points of improvement in the calculations, probably the potential model.

CONCLUSIONS

Molecular simulation shows that the presence of an ester functional group in the alkyl chain of imidazolium ionic liquids does not modify severely the local structure of the ionic liquids: the segregation between polar and nonpolar domains is similar to that observed in alkyimidazolium ILs, even if the size of these domains is affected. In the ionic liquids studied, the relative size of the domains is influenced also by the nature of the anion. The alkyl chains of the cations and those of the octylsulfate anion tend to aggregate. The presence of the ester group in the ionic liquids modifies significantly the arrangement of the anions around the cations. In alkyimidazolium ILs, the anions tend to be found near of the imidazolium ring, whereas in the ester-functionalized ILs, there is a competition between the imidazolium ring and the polar ester group to be located near the anion. This difference can influence the solvation of polar and nonpolar compounds and can explain the different performance of these functionalized ionic liquids when they are used as reaction media.

Concerning the solvation of gases, CO_2 interacts with both the most charged regions of the ILs and the nonpolar regions. We do not observe a strong affinity of the CO_2 molecule for the ester group, just in the case of the IL with the octylsulfate anion. The strong correlation between the anion and the ester group allows the CO_2 to be found also near the ester functionality. Ethane interacts preferentially with the alkyl chains of the ionic liquids. Our calculations of gas solubility using molecular simulation

agree with the experimental results of Deng et al.,¹⁷ providing a molecular interpretation of the effect of the ester group in the solubility of gases in ILs. It is shown here that, in agreement with the experimental studies, the presence of ester functionalities in the side chain of alkylimidazolium ionic liquids has a minor effect on ethane and carbon dioxide solubility.

AUTHOR INFORMATION

Corresponding Author

*Phone: +33473407205. Fax: +33 473405328. E-mail: margarida.c.gomes@univ-bpclermont.fr.

ACKNOWLEDGMENT

The participation of A.S.P. was made possible by an Ánxeles Alvariño Fellowship from Xunta de Galicia, Spain.

REFERENCES

- (1) Wassercheid, P.; Welton, T. *Ionic Liquids in Synthesis*, 2nd ed.; Wiley-VCH: 2008.
- (2) Welton, T. *Chem. Rev.* **1999**, *99*, 2071.
- (3) Zhou, F.; Liang, Y.; Liu, W. *Chem. Soc. Rev.* **2009**, *38*, 2590.
- (4) Qu, J.; Blau, P.; Dai, S.; Luo, H.; Meyer, H. *Tribol. Lett.* **2009**, *35*, 181.
- (5) Stracke, M.; Migliorini, M.; Lissner, E.; Schrekker, H.; Dupont, J.; Gonçalves, R. *Appl. Energy* **2009**, *86*, 1512.
- (6) Luo, L.; Yu, N.; Tan, R.; Jin, Y.; Yin, D.; Yin, D. *Catal. Lett.* **2009**, *130*, 489.
- (7) Mallet, J.; Molinari, M.; Martineau, F.; Delavoie, F.; Fricoteaux, P.; Troyan, M. *Nano Lett.* **2008**, *8*, 3468.
- (8) Gathergood, N.; García, M. T.; Scammells, P. J. *Green Chem.* **2004**, *6*, 166.
- (9) Latala, A.; Nedzi, M.; Stepnowski, P. *Green Chem.* **2010**, *12*, 60.
- (10) Latala, A.; Nedzi, M.; Stepnowski, P. *Green Chem.* **2009**, *11*, 580.
- (11) Latala, A.; Nedzi, M.; Stepnowski, P. *Green Chem.* **2009**, *11*, 1371.
- (12) Coleman, D.; Gathergood, N. *Chem. Soc. Rev.* **2010**, *39*, 600.
- (13) Howard, P. H.; Boethling, R. S.; Stiteler, W.; Meylan, W.; Beauman, J. *Sci. Total Environ.* **1991**, *109*, 635.
- (14) Boethling, R. S. *Cationic Surfactants*; Surfactant Science Series; Marcel Dekker: New York, 1994; Vol. 53; p 95.
- (15) Bouquillon, S.; Courant, T.; Dean, D.; Gathergood, N.; Morrissey, S.; Pegot, B.; Scammells, P. J.; Singer, R. D. *Aust. J. Chem.* **2007**, *60*, 843.
- (16) Morrissey, S.; Pegot, B.; Coleman, D.; García, M. T.; Ferguson, D.; Quilty, B.; Gathergood, N. *Green Chem.* **2009**, *11*, 475.
- (17) Deng, Y.; Morrissey, S.; Gathergood, N.; Delort, A. M.; Husson, P.; Costa Gomes, M. F. *ChemSusChem* **2010**, *3*, 377.
- (18) Deschamps, J.; Costa Gomes, M. F.; Pádua, A. A. H. *ChemPhysChem.* **2004**, *5*, 1049.
- (19) Canongia Lopes, J. N.; Pádua, A. A. H.; Shimizu, K. *J. Phys. Chem. B* **2008**, *112*, 5039.
- (20) Canongia Lopes, J. N.; Pádua, A. A. H. *J. Phys. Chem. B* **2004**, *108*, 16893.
- (21) Cornell, W. D.; Cieplak, P.; Bayly, C. I.; Gould, I. R.; Merz, K. M.; Fergusin, D. M.; Spellmeyer, D. C.; Fox, T.; Caldwell, J. W.; Kollman, P. A. *J. Am. Chem. Soc.* **1995**, *117*, 5179.
- (22) Jorgensen, W. L.; Maxwell, D. S.; Tirado-Rives, J. *J. Am. Chem. Soc.* **1996**, *118*, 11225.
- (23) Smith, W.; Forester, T. R. DL_POLY Molecular Simulation Package, 2007.
- (24) Harris, J. G.; Yung, K. H. *J. Phys. Chem.* **1995**, *99*, 12021.
- (25) Almantariotis, D.; Gefflaut, T.; Pádua, A. A. H.; Coxam, J.-Y.; Costa Gomes, M. F. *J. Phys. Chem. B* **2010**, *114*, 3608.
- (26) Widom, B. *J. Chem. Phys.* **1963**, *39*, 2808.
- (27) Mezei, M. *J. Chem. Phys.* **1987**, *86*, 7084.
- (28) Del Pópolo, M. G.; Voth, G. A. *J. Phys. Chem. B* **2004**, *108*, 1744.
- (29) Wang, Y.; Voth, G. A. *J. Am. Chem. Soc.* **2005**, *127*, 12192.
- (30) Canongia Lopes, J. N.; Pádua, A. A. H. *J. Phys. Chem. B* **2006**, *110*, 3330.
- (31) Russina, O.; Triolo, A.; Gontrani, L.; Caminiti, R.; Xiao, D.; Hines, L. G., Jr.; Bartsch, R. A.; Quitevis, E. L.; Plechkova, N.; Seddon, K. R. *J. Phys.: Condens. Matter* **2009**, *21*, 424121.
- (32) Triolo, A.; Russina, O.; Fazio, B.; Triolo, R.; Di Cola, E. *Chem. Phys. Lett.* **2008**, *457*, 362.
- (33) Triolo, A.; Russina, O.; Bleif, H.-J.; Di Cola, E. *J. Phys. Chem. B* **2007**, *111*, 4641.
- (34) Canongia Lopes, J. N.; Costa Gomes, M. F.; Pádua, A. A. H. *J. Phys. Chem. B* **2006**, *110*, 16816.
- (35) Zhang, X.; Huo, F.; Liu, Z.; Wang, W.; Shi, W.; Maginn, E. J. *J. Phys. Chem. B* **2009**, *113*, 7591.
- (36) Cadena, C.; Anthony, J. L.; Shah, J. K.; Morrow, T. I.; Brennecke, J. F.; Maginn, E. J. *J. Am. Chem. Soc.* **2004**, *126*, 5300.
- (37) Kazarian, S. G.; Briscoe, B. J.; Welton, T. *Chem. Commun.* **2000**, 2047.
- (38) Kanakubo, M.; Umecky, T.; Hiejima, Y.; Aizawa, T.; Nanjo, H.; Kameda, Y. *J. Phys. Chem. B* **2005**, *109*, 13847.
- (39) Anthony, J. L.; Anderson, J. L.; Maginn, E. J.; Brennecke, J. F. *J. Phys. Chem. B* **2005**, *109*, 6366.
- (40) Gutowski, K. E.; Maginn, E. J. *J. Am. Chem. Soc.* **2008**, *130*, 14690.
- (41) Wappel, D.; Grönald, G.; Kalb, R.; Draxler, J. *Int. J. Greenhouse Gas Control* **2010**, *4*, 486.
- (42) Hasib-ur-Rahman, M.; Sijaj, M.; Larachi, F. *Chem. Eng. Process.* **2010**, *49*, 313.
- (43) Hong, G.; Jacquemin, J.; Deetlefs, M.; Hardacre, C.; Husson, P.; Costa Gomes, M. F. *Fluid Phase Equilib.* **2007**, *257*, 27.
- (44) Jacquemin, J.; Husson, P.; Majer, V.; Costa Gomes, M. F. *J. Solution Chem.* **2007**, *36*, 967.
- (45) Costa Gomes, M. F.; Pádua, A. A. H.; Pensado, A. S.; Pison, L. Using Light Hydrocarbons To Probe the Structure of Imidazolium Based Ionic Liquids; COIL-3, 2009, Cairns, Australia.
- (46) Dunning, T. H., Jr. *J. Chem. Phys.* **1989**, *90*, 1007.
- (47) Annappureddy, H. V. R.; Kashyap, H. K.; De Biase, P. M.; Margulis, C. J. *J. Phys. Chem. B* **2010**, *114*, 16838.